Applied Catalysis B: Environmental 88 (2009) 194–203

Contents lists available at ScienceDirect

Applied Catalysis B: Environmental

journal homepage: www.elsevier.com/locate/apcatb

Effect of sample preparation and humidity on the photodegradation rate of CEES on pure and Zn doped anatase TiO_2 nanoparticles prepared by homogeneous hydrolysis

Lars Österlund [a,*], Václav Štengl [b], Andreas Mattsson [a], Snejana Bakardjieva [b], Per Ola Andersson [a], František Opluštil [c]

[a] FOI CBRN Defence and Security, SE-901 82 Umeå, Sweden
[b] Institute of Inorganic Chemistry AS CR v.v.i., 250 68 Řež, Czech Republic
[c] Military Technical Institute of Protection Brno, Veslařská 230, 637 00 Brno, Czech Republic

ARTICLE INFO

Article history:
Received 30 May 2008
Received in revised form 19 September 2008
Accepted 26 September 2008
Available online 9 October 2008

Keywords:
CEES
TiO_2
Photocatalysis
Homogeneous hydrolysis
Diffuse reflectance
Fourier transform infrared spectroscopy

ABSTRACT

Pure titania and titania doped with Zn^{2+} were prepared by homogeneous hydrolysis in aqueous solution with urea and thioacetamide as precipitating agents. The materials were characterized by XRD, TEM, BET and BJH analysis, which show microporous, nanaocrytsalline anatase phase titania in the size range 4–5 nm and specific surface area 200–500 m^2/g. Adsorption and photocatalytic decomposition of 2-chloroethyl ethyl sulfide (CEES) was measured on dry and water pre-covered titania surfaces, respectively. Illumination with UV light leads to rapid decomposition of CEES on all samples resulting in formation of surface bound ethoxy, chloro ethoxy, aldehydes, acetone and carboxylates. Volatile sulphur moieties (S=O) and isocyanate (Ti-NCO) are observed which is related to the synthesis methods employed. A procedure for removing residual synthesis products from the particles was devised and the intrinsic photodegradation rate was determined on the purified samples and compared with the as prepared samples. The photodegradation rate is notable higher for the purified TiO_2 nanoparticles prepared by the urea route with respect to the "as prepared". In the case of the Zn doped TiO_2 samples a diminution in photodegradation rate is observed after purification. The results are correlated with the amount of volatile residual synthesis products present on the different particles. All materials have comparable or higher photo-reactivity than P25 (Degussa). On a humidified surface, the effects from synthesis residues, in particular volatile sulphur moieties, are reduced due to reactions with water and improved photoreaction rates for all samples are observed.

1. Introduction

Photocatalytic decomposition of pollutants on wide band gap semiconducting metal oxides and in particular TiO_2 nanoparticles is a promising remediation technology, which has advanced significantly during the past two decades [1–6]. Several authors have reported the use of TiO_2 for photocatalytic degradation of toxic chemicals, including chemical warfare agents (CWA) [7–9]. The latter is interesting since available decontamination technology suffers from several disadvantages such as large volume of degassing solutions or toxic by-products, which require post-treatment methods. Several problems have however been encountered when evaluating the efficiency of TiO_2 for CEES degradation including build up of inorganic sulphur on the catalyst surface and gradual deterioration of the activity which necessitates catalyst regeneration [7,8].

In view of the hazards of CWA, simile agents with similar chemical properties are usually employed in research. 2-Chloroethyl ethyl sulfide (CEES) is a simile substance for sulphur mustard gas, HD (2,2-dichloroethyl sulfide). It possesses both S-group and Cl-group functionality which makes its chemistry more complex than simile molecules containing single reactive groups, e.g. opening up competing pathways for charge transfer. It has recently been reported that electron transfer from the TiO_2 conduction band occurs only into the Cl-group [10].

Considerable efforts have been exerted to develop new and cost-effective preparation methods of titania and doped titania with enhanced photocatalytic properties [6,11,12]. Homogeneous

* Corresponding author. Tel.: +46 90 106900; fax: +46 90 106800.
E-mail address: lars.osterlund@foi.se (L. Österlund).

0926-3373/$ – see front matter © 2008 Elsevier B.V. All rights reserved.
doi:10.1016/j.apcatb.2008.09.029

precipitation with urea in aqueous solution for preparation of spherical particles of photocatalytic ferrihydrite [13], photocatalytic anatase [14], nanosized TiO_2 or ferrihydrite for decomposition of CWA [15] and pigments based on mica coated with oxides of metal [16] have previously been prepared by us and others [17]. The decomposition of urea (CH_4N_2O) in aqueous solution is accompanied by slow and controlled supply of ammonia (NH_3) and carbon dioxide (CO_2) into solution. The smooth pH increase obtained by the degradation of urea with the concerted release of OH^- and CO_3^{2-} ions, usually leads to the precipitation of metal hydrous oxide particles of controlled particle morphology [18]. All microstructural parameters as particle shape and size, specific surface area and porosity are quite sensitive towards pH, metal ion concentration, temperature and aging time. In the same way as the urea method, homogeneous precipitation of metal sulphides by thermal decomposition of thioacetamide (TAA) is also a viable method to prepare metal oxide nanoparticles [19]. Thioacetamide releases hydrogen sulphide at a temperature higher than 60 °C in acidic solution. The reaction products (MeS) are nanosized spherical particles with a well-developed microstructure, but different from homogeneous precipitation with urea. Such materials can be produced with high specific surface area [20]. Homogeneous precipitations with thioacetamide for TiO_2/ZnS nanocomposites [21] and TiO_2/ZnO nanocomposites [22] have been reported elsewhere.

An additional question to be addressed when sulphate precursors are used in the particle synthesis is whether these influence the ultimate reactivity of the materials. It is known that the presence of sulphur in titania increases its surface acidity by introducing Brönsted acid sites due to formation of e.g. hydrogen sulphate ions (HSO_4^-) and strengthening existing Lewis acid sites (Ti^{4+}) [23]. Similarly, it expected that the humidity plays a critical role for the surface reactivity as a source of hole acceptor (hydroxyls), competing for adsorption sites, and for establishing equilibrium reaction kinetics [2,3,24].

In this paper, we present results of the synthesis and characterization of titania and Zn doped titania prepared by homogeneous precipitation with urea and thioacetamide, respectively, in aqueous solution. We present a diffuse reflectance Fourier transform infrared spectroscopy (DRIFTS) study of the adsorption and photo-assisted decomposition of CEES on the various titania samples. We report on differences in the DRIFT spectra for the different synthesis methods, pure vs. Zn doped titania and dry vs. wet surfaces, respectively and the influence of synthesis route and pretreatment method on the reactive properties on the final materials.

2. Experimental

2.1. Preparation of samples

The nanocrystalline anatase TiO_2 prepared by hydrolysis of $TiOSO_4$ aqueous solutions using urea as the precipitation agent (sample denoted as Ti_TU) was prepared as follows: $TiOSO_4$ (30 g) was dissolved in 100 ml hot water acidified with 10 ml of 98% H_2SO_4. The pellucid liquid was diluted into 4 L of distilled water and mixed with 200 g of urea. The mixture was heated to 100 °C under stirring and kept at this temperature for 6 h until pH 7 was reached and releasable ammonia escaped from the solution [14]. Anatase doped with Zn^{2+} using the urea route was prepared of mixture of 30 g $TiOSO_4$ and 5 g $ZnSO_4{\cdot}7H_2O$ by homogeneous hydrolysis with 200 g of urea (sample denoted as TiZn_TU) [27]. The pure and Zn doped anatase TiO_2 samples prepared with thioacetamide as the precipitation agent was prepared as follows: First 100 g of $TiOSO_4$ was dissolved in 4 L water acidified with of 98% H_2SO_4 to pH 2 (sample denoted Ti_TAA) and secondly 85 g $TiOSO_4$ and 15 g $ZnSO_4{\cdot}7H_2O$ was dissolved in 4 L water acidified with of 98% H_2SO_4 to pH 2 (sample denoted as TiZn_TAA). Subsequently 100 g thioacetamide was added. The reaction mixture was heated at 100 °C under stirring for 4 h [20,21]. Sample denoted Ti_TAAU was prepared by a combination of both methods, i.e. urea and thioacetamide homogenous hydrolysis. Briefly, 100 g $TiOSO_4$ was heated for 2 h with 50 g thioacetamide at pH 2 and then 200 g urea was added. The reaction mixture was heated at temperature 100 °C until pH 7 was reached and ammonia escaped from the solution. All synthesized samples were washed by distilled water, filtered off and dried at 105 °C in oven. Prepared samples were characterized, for details see below. Material characteristics of the prepared samples are summarised in Table 1.

2.2. Characterization methods

Scanning electron microscopy (SEM) studies were performed using a Philips XL30 CP microscope equipped with EDX (energy dispersive X-ray), Robinson, SE (secondary electron) and BSE (back-scattered electron) detectors. The sample was placed on an adhesive C slice and coated with Au–Pd alloy 10 nm thick layer.

High-resolution transmission electron microscopy (HRTEM) was done with transmission electron microscope JEOL JEM 3010 operated at 300 kV (LaB6 cathode) giving a point resolution of 0.17 nm. A copper grid coated with a holey carbon support film was used to prepare samples for the TEM observation. A powdered sample was dispersed in ethanol and the suspension was treated in ultrasonic bath for 10 min.

The surface area of the samples was determined from nitrogen adsorption–desorption isotherms at liquid nitrogen temperature using a Coulter SA3100 instrument with outgas 15 min at 120 °C. The BET method was used for surface area calculation [25], and the pore size distribution (pore diameter and pore volume of the samples) was determined by the BJH method [26].

2-Chloroethyl ethyl sulphide (CEES; 98% GC purity, Sigma Aldrich). CEES was used as delivered and loaded in a dedicated gas generator, as described elsewhere [28,29]. The liquid was heated to 62 °C and evaporated into a gas stream of synthetic air (80% N_2 and 20% O_2 with 99.994% respectively 99.999% gas purity) through a diffusion tube. The calibrated steady state CEES evaporation rate was determined to be 17.0 $\mu g\,min^{-1}$. Calibration was done by determine the weight loss of CEES with 100 ml/min synthetic air flow after an extended dosing time, ~46 h. The reaction gas was subsequently fed into the reaction cell through heated gas tubes

Table 1
Compilation of materials data and their physical properties.

Sample denotation	Precipitating agent	Contents of $ZnSO_4{\cdot}7H_2O$ in reaction mixture (wt.%)	Specific area ($m^2\,g^{-1}$)	Pore volume distribution ($cm^3\,g^{-1}$)	Particle size from TEM (nm)
Ti_TU	Urea	–	291	0.244	7–8
Ti_TAA	Thioacetamide	–	160	0.057	8–10
Ti_TAAU	Urea + thioacetamide	–	277	0.024	20–25
TiZn_TU	Urea	15	432	0.326	10–12
TiZn_TAA	Thioacetamide	15	20	0.025	19–20

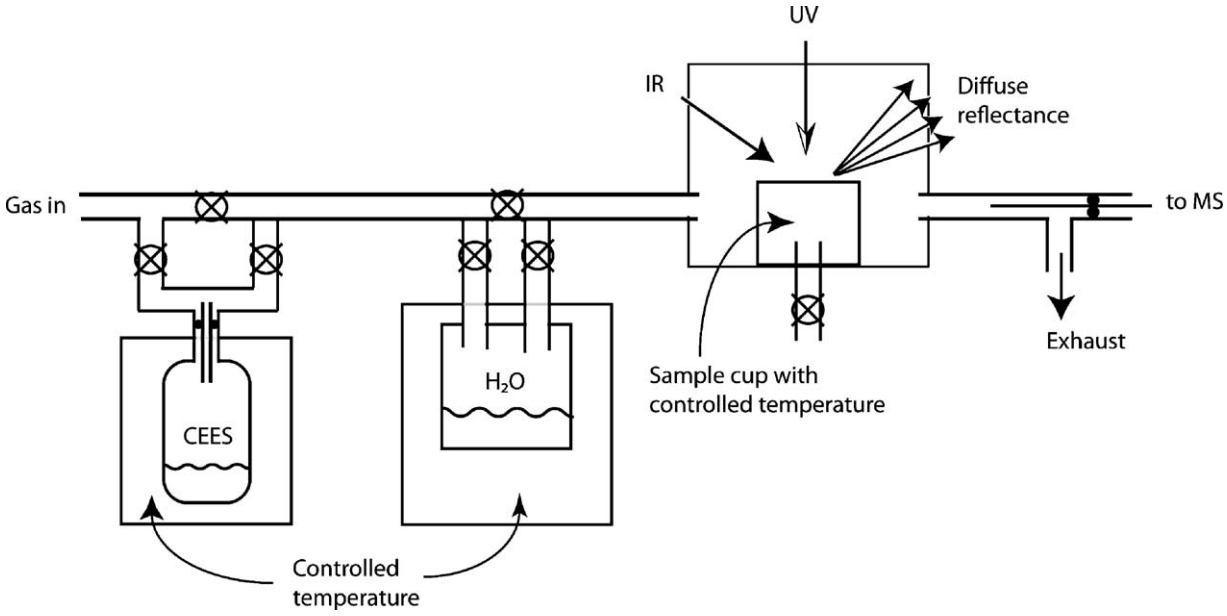

Fig. 1. Schematic drawing of the experimental set-up for in situ DRIFT spectroscopy.

($T \sim 65$ °C) to reduce condensation of CEES on the tube walls. Dosing of the reaction gas was done by first dosing CEES for 15–25 min, and then flushing the cell with pure synthetic air for 15 min. No other gases than CEES, N_2, O_2, and H_2O and trace levels of residual gases were detected mass spectrometrically (QMG422, Pfeiffer Vacuum).

DRIFT spectra were acquired with a vacuum pumped Fourier transform infrared spectrometer (Bruker IFS 66 v/S) equipped with a modified in situ reaction cell allowing for simultaneous DRIFT spectroscopy, on-line mass spectrometry and light illumination [28,29]. Repeated in situ DRIFT spectra were acquired as a function of time by collecting 68 scans (30 s) followed by 30 s dwell time between consecutive spectra. Post-treatment of the spectra included smoothing with the Savitzky-Golay method using a 9 data point window and baseline corrections. The spectra are presented in absorbance units ($\log(1/R)$) to allow for discrimination of both increasing and decreasing absorption bands compared to the background spectrum. Prior to each new measurement, the samples were annealed at 400 °C for 15 min in synthetic air. For DRIFT spectra in humid environments the samples was exposed to humidified air (relative humidity, RH = 17% at 21 °C) for 15 min followed by 20 min of dry air. Dosing of CEES was then done in the same manner as for the measurements in a dry environment. A schematic of the experiment set-up is given in Fig. 1.

To investigate effect of impurities on the different synthesis protocols employed in the present study a set of samples from the Ti_TU, Ti_TAA, TiZn_TU and TiZn_TAA batches were in addition calcinated at 440 °C for 24 h and/or washed in 1 mM NaOH prior to the photodegradation experiments. A fairly low calcination temperature was applied to avoid particle sintering [23]. Before the calcination, the sample colours were ranging from white to pale sienna. After calcination all samples were completely white with exception of the Ti_TAA sample which maintained a slight yellowish colouration, which became slightly grey/lilac upon NaOH washing.

Photodegradation of simile agents was done with a 200 W Hg(Xe) high-pressure arc lamp, which was coupled to the reaction cell through a fibre optical bundle [29]. The infrared part of the lamp source spectrum was blocked by a 75 mm water filter to reduce sample heating. No other filters were used in the experiments. The measured photon power at the sample surface was 166 mW/cm^2 and ~19 mW/cm^2 in the wavelength regions $200 < \lambda < 800$ and $200 < \lambda < 400$ (UV region), respectively, as measured with a calibrated thermopile detector.

3. Results and discussion

3.1. Physical characterization of TiO_2 nanoparticles

In Fig. 2 are depicted electron micrographs of samples prepared according to the procedures described above. The SEM micrographs show roughly spherical particles that are ~2 μm in size. HRTEM microphotographs (Fig. 3) show that the agglomerates observed in SEM consist of primary nanoparticles with a mean diameter $\langle d \rangle$ between 7 and 25 nm (Table 1) depending on preparation method and the extent of Zn doping. The TiO_2 particles prepared with thioacetamide (Fig. 3b) contain significantly larger amorphous domains than do the particles prepared with urea (Fig. 3a). This is also the case when Zn is co-added to the particles (Fig. 3c and d). The SAED diffraction patterns show that the individual particles have well-developed crystallinity with the anatase modification. This is further corroborated by the XRD data which show the characteristic 2Θ values of the diffraction peaks for anatase crystals (ICDD PDF card 21-1272). No other polymorph of titania are observed.

The specific surface area (BET) of all prepared samples, obtained from the N_2 adsorption isotherms, was determined to be between 200 and 500 m^2 g^{-1} depending on preparation method used (Table 1). We note that the low surface area of the TiZn_TAA sample is correlated with a well-devolved crystallinity seen in TEM, and small pore volume distribution. The samples displayed a type I isotherm with desorption hysteresis loop A. Type A hysteresis is principally due to cylindrical pores open at both ends and the microporosity of the pore size distribution indicates a pore diameter <6 nm. The results from desorption BJH pore volume distribution and pore area distribution analysis confirmed the microporous structure of all prepared samples [14,16,20,21].

3.2. Influence of nanoparticle synthesis methods

From Fig. 4 it is apparent that the DRIFT spectra after CEES adsorption are qualitatively different depending on whether the

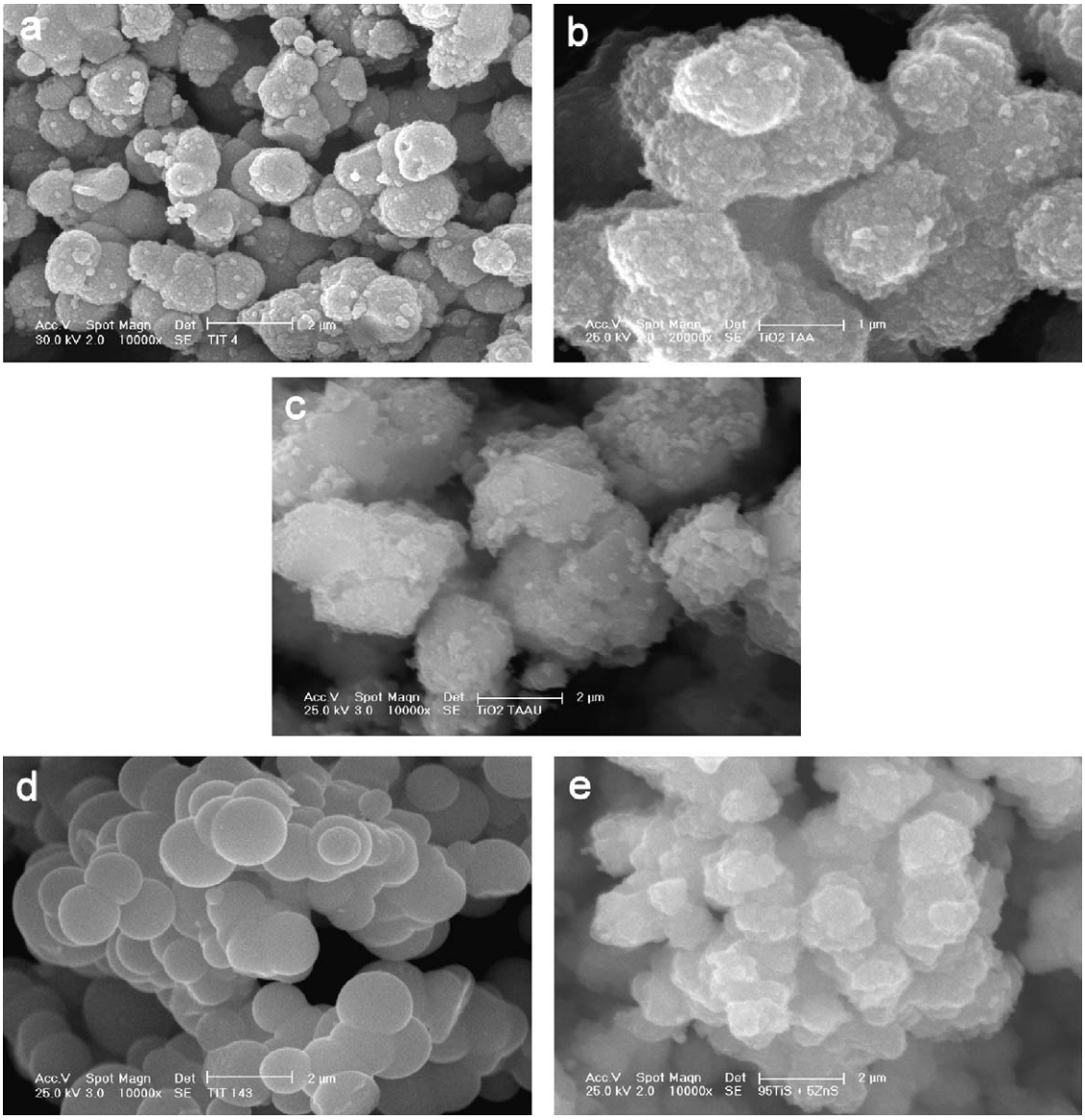

Fig. 2. SEM micrographs of samples denoted as (a) Ti_TU, (b) Ti_TAA, (c) Ti_TAAU, (d) TiZn_TU and (e) TiZn_TAA (*cf.* Table 1).

thioacetamide or urea synthesis route is employed. It is evident that the δ(HOH) water bending mode at 1620–1630 cm^{-1} increases (synchronously with the ν(OH) modes at ~3200 cm^{-1}, not shown) on titania prepared with urea (Ti_TU and to some extent Ti_TAAU), while it decreases on samples prepared with thioacetamide (Ti_TAA). This indicates facile water displacement on Ti_TAA. Furthermore, in Fig. 4 it is seen that pronounced negative absorption bands (indicating decreasing concentration of absorbing species) appear in the 1400–1600 cm^{-1} region and at ca. 1360 cm^{-1} for the samples prepared with urea and thioacetamide, respectively, directly after dosing CEES. The negative bands become more pronounced during UV illumination. This suggests that CEES molecules react with volatile surface moieties and chemically transform them so that their chemical signatures (absorbance) effectively diminish. Subsequently these species are successively depleted upon UV illumination. Upon illumination the negative absorption bands at 1400–1600 cm^{-1} present on samples prepared with urea (spectra (a)) successively becomes more pronounced while simultaneously a new absorbance band appears at 2202 cm^{-1}. We attribute the latter band to the ν(NCO) mode in isocyanate (Ti-NCO) formed from photoreaction of urea residues (with typical frequencies in the 1400–1600 cm^{-1} regime) since it is only seen on samples synthesized with urea [30,31].

In Fig. 5a and b are shown DRIFT spectra obtained after CEES dosing on pure TiO_2 prepared with urea and thioacetamide, respectively, after extended calcination (Fig. 5a) and/or NaOH washing (Fig. 5b). Long time calcination at 440 °C of TiO_2 made by the TAA route does not alter the DRIFT spectra significantly (Fig. 5b). However, subsequent washing (1 mM NaOH) effectively removes all negative bands on the pure TiO_2 sample. In fact, only washing in NaOH is sufficient to remove the negative absorption bands. NaOH washing shifts the 1360 cm^{-1} band ca. 15 cm^{-1} towards lower wavenumbers, which probably is due to Na binding to the surface. It has been suggested by Hauck et al. [31] in an in situ IR photocatalytic study of isocyanic acid adsorption on anatase TiO_2 that a similar sharp 1360 cm^{-1} dip originates from the ν(S=O) vibration of sulphate species originating from the synthesis procedure of the titania samples. During the in situ experiments reported in that study these sulphate species interact with H_2O and subsequently disappear from the TiO_2 surface.

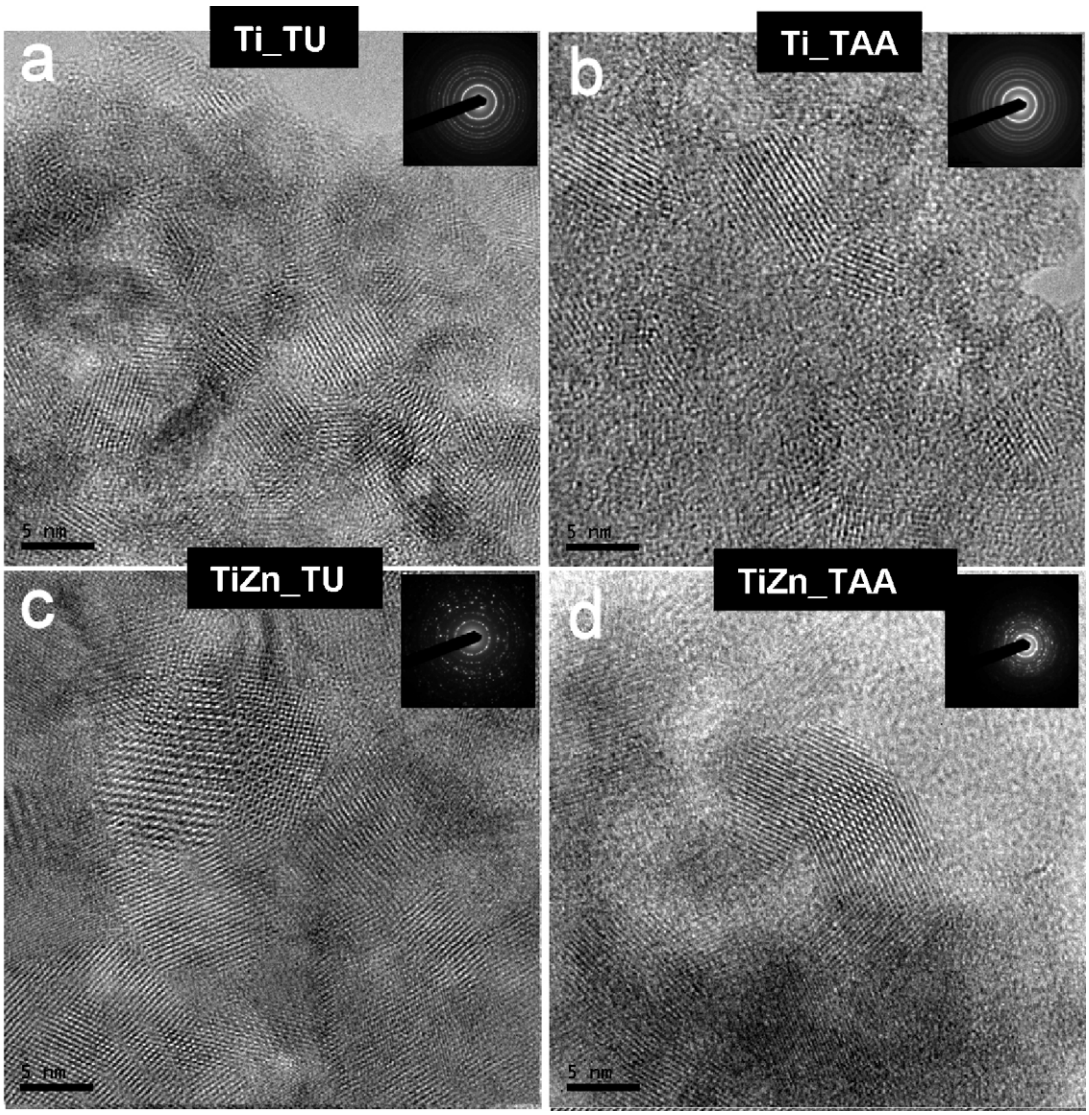

Fig. 3. HRTEM micrographs of sample (a) Ti_TU, (b) Ti_TAA, (c) TiZn_TU and (d) TiZn_TAA (*cf.* Table 1).

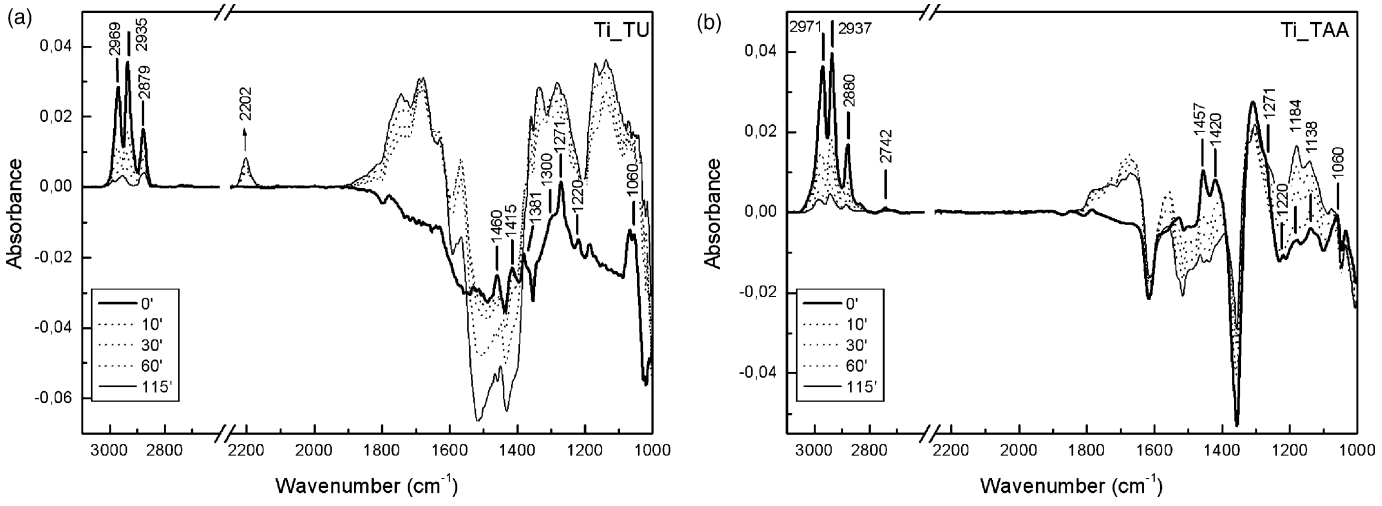

Fig. 4. DRIFT spectra of samples Ti_TU (a) and Ti_TAA (b) measured in synthetic air after CEES adsorption. The shown spectra are acquired prior to illumination and after 10, 30, 60 and 115 min of UV illumination, respectively. The arrow indicate growth Ti–NCO absorbance vs. illumination time.

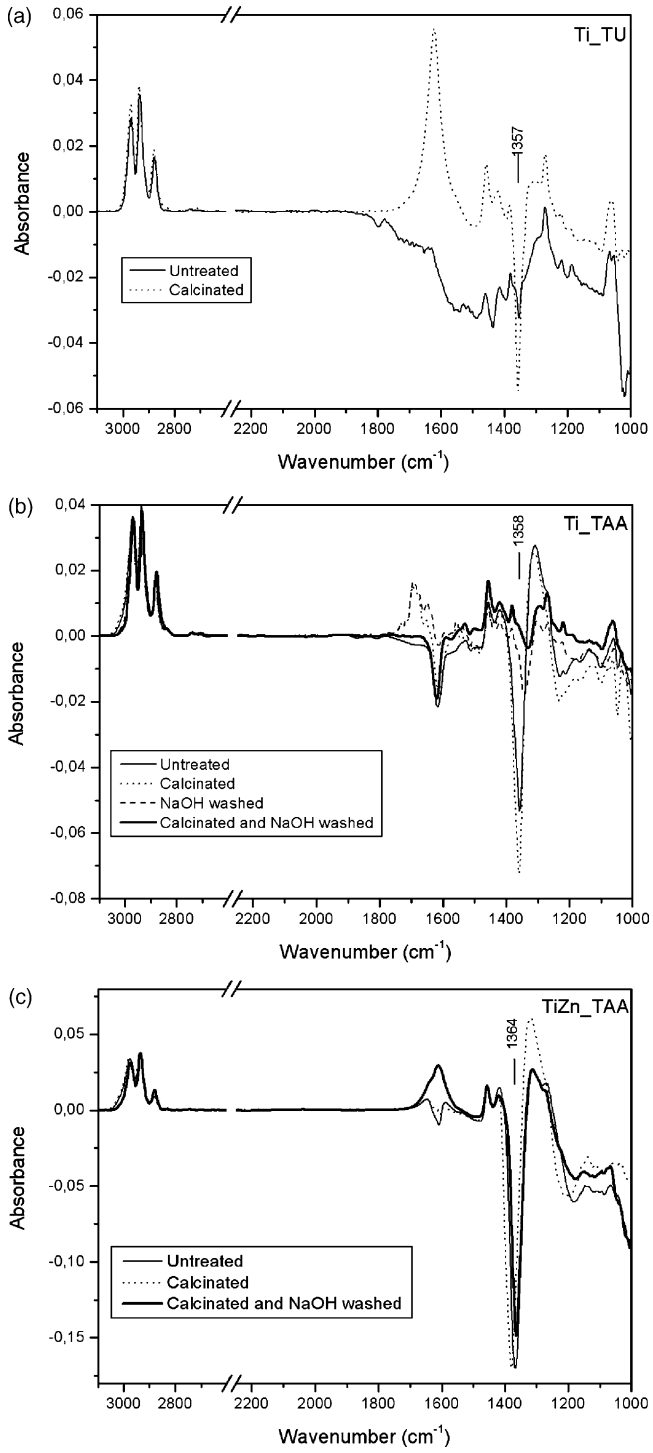

Fig. 5. DRIFT spectra of Ti_TU (a), Ti_TAA (b) and TiZn_TAA (c) after CEES adsorption in synthetic air. Measurements are done on as prepared, calcinated, NaOH washed, and calcinated and washed samples.

For samples prepared via the urea route only extended calcination is sufficient to remove urea residues from TiO_2. It is evident that the 2204 cm^{-1} absorbance is depleted for both pure and Zn doped samples (see Figs. 6a and 7a below). A colour change from light yellow to white of the sample further support that removal of strongly bonded urea residues during the pro-longed calcination. However, in the case of TiO_2 prepared via the urea route (Ti_TU) extended calcination leads to concerted evolution of a negative absorption bands at 1360 cm^{-1} (Fig. 5a). Martín et al. [23] studied the effect of surface chemical properties of titania prepared by the sulphate route (as in our case) and showed that annealing leads to surface segregation of sulphate and formation of volatile sulphate surface species. They also discovered Na content on the sample after NaOH wash. It is therefore reasonable to assume that our extended calcination pretreatment procedure leads to similar formation of volatile sulphate species on Ti_TU. Thus moderate calcination is appropriate to recover pure TiO_2 particles prepared by the urea route.

In Fig. 5c is shown corresponding experiments for Zn doped TiO_2 (TiZn_TAA). The negative absorption band that appears at ca 1360 cm^{-1} for pure TiO_2 shifts towards higher wavenumbers with Zn content. For the Zn doped samples the absorbance loss at 1360 cm^{-1} appears independent on pretreatment (washing and/or calcination); only a minor decrease of the 1360 cm^{-1} is observed after NaOH washing. This indicates that sulphate residues are more strongly bonded on Zn doped TiO_2, which we tentatively attribute to Zn–S bond formation.

We thus conclude that the negative absorption band at ~1360 cm^{-1} seen in Fig. 5 (also seen in Fig. 4) is due to volatile sulphate surface species originating from either the $TiOSO_4$ precursor (urea route) or the precipitating agent (thioacetamide route). In the latter case both Zn–S bond formation in the Zn doped TiO_2 prohibits removal of sulphate complexes by NaOH washing.

In the following we apply a 'pretreatment' procedure (calcination and/or NaOH washing) to each of the sample series to remove spurious synthesis residues prior to CEES adsorption and photodegradation experiments. We consistently apply NaOH washing on the Zn doped samples where we noted stronger bonding of organic residues. We compare the results thus obtained with those in Fig. 4 on the 'as prepared' samples.

3.3. Photodegradation of CEES in dry environment

3.3.1. TiO_2

In Fig. 6 are shown DRIFT spectra obtained on samples pretreated by extended calcination (Ti_TU; urea route) and calcination + NaOH washing (Ti_TAA; thioacetamide route). In comparison with the as prepared samples the CEES spectra are more consistent with previous reports of CEES adsorption on clean TiO_2 [32]. The most pronounced peaks are the well-known absorption bands at 1040–1070 cm^{-1} due to ν(C–C), ~1220 cm^{-1} due to $\delta(CH_2S)$, ~1272 cm^{-1} due to $\delta(CH_2)$; ~1416 cm^{-1} due to $\delta(CH_2)$, and the ~1457 cm^{-1} due to $\delta(CH_3)$. In the ν(C–H) region the three most distinct stretching modes for CEES are found on all samples at approximately the same frequencies at ~2974, ~2935 and ~2880 cm^{-1}. The absorption band at 1619 cm^{-1} is due to δ(HOH) in water. Significantly more water builds up on Ti_TU than on Ti_TAA in the course of the photoreaction (the water coverage varies somewhat between experiments; this is inevitably for dried, hygroscopic samples – even in a dry synthetic gas feed). No indication of thermal dissociation of CEES is observed on samples Ti_TU and Ti_TAA, while after CEES adsorption on the as prepared Ti_TAA sample (Fig. 4) C–O complexes form which have vibrational signatures in the 1100–1200 cm^{-1} region indicating S–C bond fission. Typically these species are ethoxy and chloroethoxy groups bonded to Ti surface atoms [32,33]. These results suggest nucleophilic attack by volatile TAA derived surface moieties on the as prepared Ti_TAA sample.

All absorption bands associated with CEES decreases upon illumination. A number of oxidation intermediates are produced during the photoreaction. Typical carbonyl absorption bands can be seen between 1660 and 1730 cm^{-1}. Interestingly, the absorption

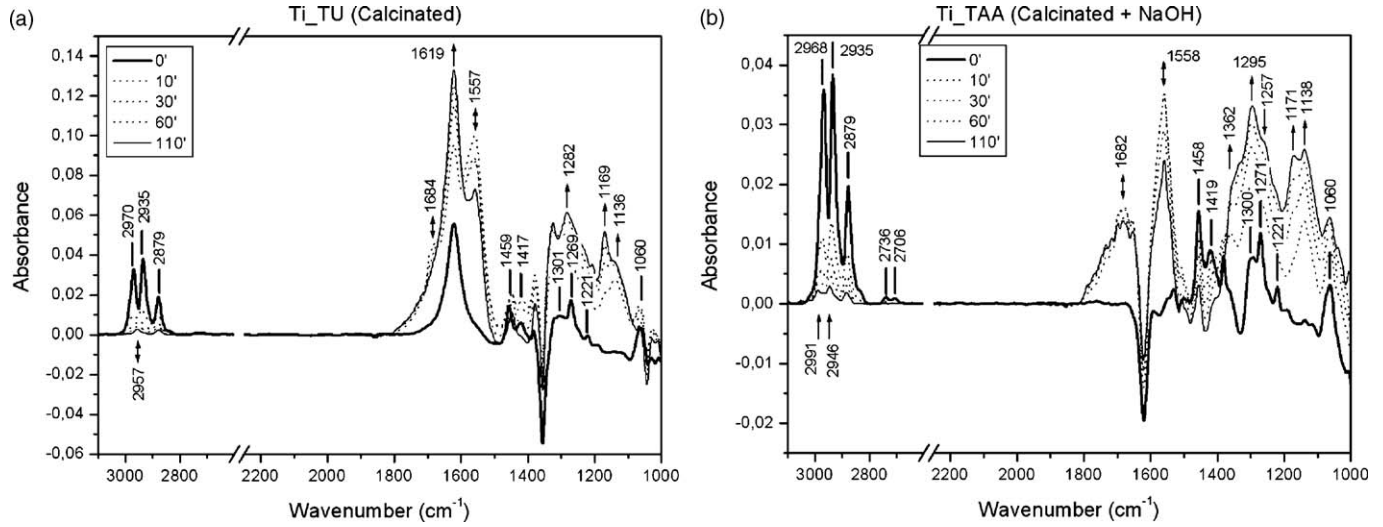

Fig. 6. DRIFT spectra of CEES adsorbed on (a) Ti_TU pretreated by extended calcination and (b) Ti_TAA pretreated by extended calcination and NaOH washing in synthetic air. Spectra shown are prior to illumination and after 10, 30, 60 and 110 min of UV illumination, respectively, in synthetic air. The arrows indicate growth or decline of absorbance vs. illumination time.

bands at ~1691 cm^{-1} and ~2991 cm^{-1} that appear after some time of UV illumination on Ti_TAA correlate and is tentatively assigned to acetone which is a common intermediate of alkane photooxidation [34]. The appearance of the peak at ~2954 cm^{-1} is due to the well-known $\nu_s(COO) + \delta(CH_3)$ combination band in formate, which follows the appearance of the corresponding ~1566 and ~1361 cm^{-1} peaks due to $\nu_s(COO)$ and $\delta(CH_3)$, respectively. During CEES decomposition ethoxy and chloroethoxy groups bonded to the Ti surface form. These complexes can be found in the region between 1100 and 1200 cm^{-1} [32].

3.3.2. Zn doped TiO_2

The DRIFT spectra on Zn doped TiO_2 pretreated with extended calcination and NaOH washing are shown in Fig. 7. The spectra appear qualitatively different from the pure TiO_2 samples. For TiZn_TU it is evident that total photooxidation is impeded compared to Ti_TU, contrary to the result for the as prepared samples. Intermediate absorption peaks due to ethoxy, chloroethoxy and carboxylates dominate the spectra. For reasons discussed above, it was not possible to remove sulphur moities (and the associated 1360 cm^{-1} spectral feature) from the Zn doped samples prepared by the TAA route (TiZn_TAA). The spectra appear qualitatively similar to the DRIFT spectra obtained on the as prepared Ti_TAA sample. We conclude that the photoreactions on TiZn_TAA are dominated by the photochemistry between residual TAA species and CEES.

3.3.3. CEES photodegradation kinetics in dry environment

The rate constant for CEES photodegradation was determined from the temporal evolution of the individual ν(C–H) modes at 2937 and 2971 cm^{-1}, and the integrated ν(C–H) bands. These peaks are readily resolved on all samples in contrast to those in the finger print region. The photodegradation rate is well described by first-order reaction kinetics during the initial 15 min illumination period [3]. In Tables 2 and 3 are shown the compiled values of the degradation rate constant for as prepared, calcinated and/or NaOH washed samples. In Table 2 is also shown the corresponding data for Degussa P25, which is usually used as a benchmark material. It

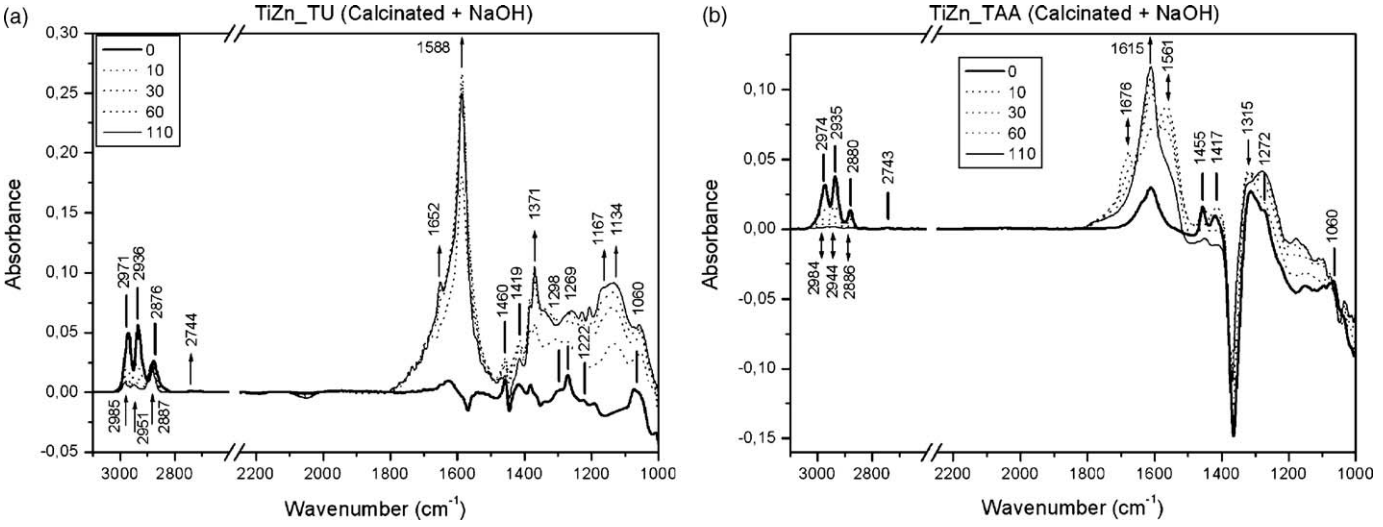

Fig. 7. DRIFT spectra of CEES adsorbed on (a) TiZn_TU pretreated by calcination and NaOH wash and (b) TiZn_TAA pretreated by extended calcination and NaOH wash. Spectra shown are prior to illumination and after 10, 30, 60 and 110 min of UV illumination, respectively, in synthetic air. The arrows indicate growth or decline of absorbance vs. illumination time.

Table 2
The CEES decomposition rate constant, $k(\nu)$, at $0 < t < 15$ min on the as prepared samples in synthetic air ("dry") and humidified synthetic air ("humid") deduced from the normalize absorbance, A, for different absorption bands.

Sample denotation	Rate constant, $k(\nu)$ (min^{-1})					
	Dry			Humid		
	ν = 2937 (cm^{-1})	ν = 2971 (cm^{-1})	$\int A(\nu)\,d\nu$ (Abs cm^{-1})	ν = 2937 (cm^{-1})	ν = 2971 (cm^{-1})	$\int A(\nu)\,d\nu$ (Abs cm^{-1})
TiZn_TU	0.112	0.114	0.072	0.155	0.124	0.104
TiZn_TAA	0.074	0.076	0.055	0.132	0.140	0.133
Ti_TU	0.074	0.086	0.051	0.124	0.125	0.078
Ti_TAA	0.070	0.080	0.057	0.101	0.114	0.100
Ti_TAAU	0.048	0.046	0.033	0.078	0.084	0.066
P25	0.075	0.083	0.051	0.055	0.056	0.034

is important to identify the rate determining steps, which determines the overall degradation rate. This requires that not only the degradation of the parent molecule is analyzed, but also decomposition products present on the surface. In Tables 2 and 3 we thus also show the degradation rate determined for the integrated ν(C–H) band. This yields a good measure of the total oxidation rate of surface bonded organics which independently was confirmed by analyzing the kinetics of the ν(C═O) and ν(COO) bands at 1660–1730 cm^{-1} and 1540–1590 cm^{-1}, respectively, for a few samples. From Tables 2 and 3 it is evident that the total degradation rates on the as prepared samples are significantly lower than for the parent molecule due to the slower degradation rate of intermediates. This is also true for the purified TiZn_TU sample. The rates of decay of individual CEES specific IR bands are also consistently faster on the as prepared samples compared to the purified samples. We attribute this to facile photo-induced CEES degradation with urea and thioacetamide residues (which are still present also on the pretreated TiZn_TAA sample). Moreover, the total photodegradation rate is consistently higher on the pure TiO_2 samples (Ti_TU and Ti_TAA) than the Zn doped samples. This contrasts the results for the as prepared samples, where an opposite result (Ti_TU vs. TiZn_TU) or comparable result (Ti_TAA vs. TiZn_TAA) was inferred. The total degradation rate on the as prepared TiO_2 samples is consistently inferior to the pretreated samples, which is attributed to slow photoreaction of synthesis residues and CEES complexes on the as prepared samples.

In contrast to the Zn doped samples the degradation rates for pure titania Ti_TU and Ti_TAA increases upon calcination. For Ti_TU calcination leads to a marked increase of the total rate by ca 120% to $k = 0.11$ min^{-1}, while for Ti_TAA only a small increase is observed (not shown). However, when Ti_TAA is further washed in NaOH it rises up to 20% ($k = 0.064$ min^{-1}). Both results correlate with the spectroscopy data in Fig. 5 and further support that the total degradation rate on TiO_2 scales with the surface impurity concentration; a decreasing impurity concentration increases the total reaction rate. We conclude that calcination is good for Ti_TU while NaOH washing is better suited for the samples prepared by the thioacetamide route. In all cases the Zn doped samples exhibit inferior activity compared to the pure TiO_2 samples, albeit comparable to P25. In particular, both pure titania samples (Ti_TU and Ti_TAA) show higher reactivity compared to P25. We attribute the lower reactivity resulting from Zn doping to strongly bonded residual organics from the particle synthesis (see Fig. 5). Our results suggest that intrinsic degradation rate (not influenced by synthetic residues) depends strongly on the sample purity, and that even small amounts of residues can significantly influence the measured reactivity (up to a factor of two). Since photodegradation of pollutants is a surface driven reaction we may expect that the observed differences of the sample cleanliness is due to several factors, such as available binding sites for CEES adsorption, which increases as synthesis residues are removed, as well as competing pathways for photo-generated radicals. Moreover, the higher intrinsic reactivity of the purified samples prepared with urea compared to thioacetamide can be correlated with HRTEM data in Fig. 3, where it is seen that Ti_TU and TiZn_TU materials contain well-resolved crystalline particles, while materials prepared with thioacetamide contain significant amorphous domains. Thus we may anticipate that with the urea route less electron–hole pair recombination centres for the photo-excited electrons are present in the final material.

3.4. CEES photodegradation on wet surfaces

The DRIFT spectra obtained on as prepared wet surfaces (Figs. 8 and 9) are qualitatively similar to those acquired on the dry samples and are also found to follow (pseudo) first-order kinetics during the first 15 min illumination time. Some very important differences can, however, be observed. The "dip" at 1360 cm^{-1} is not present on the wet surfaces, whereas the negative bands between 1400 and 1600 cm^{-1} found on Ti_TU and TiZn_TU still can be seen on the wet surfaces. This suggests that the sulphates can be removed by hydrolysis (but not by dry oxidation in synthetic air at 400 °C) in good agreement with previous reports [31]. It is also evident that the concentration of organic molecules decreases much faster on a wet surface. This is in good agreement with previous findings [28,35]. The basic

Table 3
The CEES decomposition rate constant, $k(\nu)$, at $0 < t < 15$ min on pretreated samples in synthetic air ("dry") and humidified synthetic air ("humid") deduced from the normalize absorbance, A, for different absorption bands. The samples were pretreatment at 440 °C for 24 h and washed in 1 mM NaOH prior the photodegradation experiments.

Sample denotation	Rate constant, $k(\nu)$ (min^{-1})					
	Dry			Humid		
	ν = 2937 (cm^{-1})	ν = 2971 (cm^{-1})	$\int A(\nu)\,d\nu$ (Abs cm^{-1})	ν = 2937 (cm^{-1})	ν = 2971 (cm^{-1})	$\int A(\nu)\,d\nu$ (Abs cm^{-1})
TiZn_TU	0.092	0.075	0.054	0.103	0.097	0.062
TiZn_TAA	0.031	0.034	0.031	0.062	0.067	0.062
Ti_TU	0.132	0.128	0.112	–	–	–
Ti_TAA	0.058	0.067	0.064	0.088	0.090	0.086

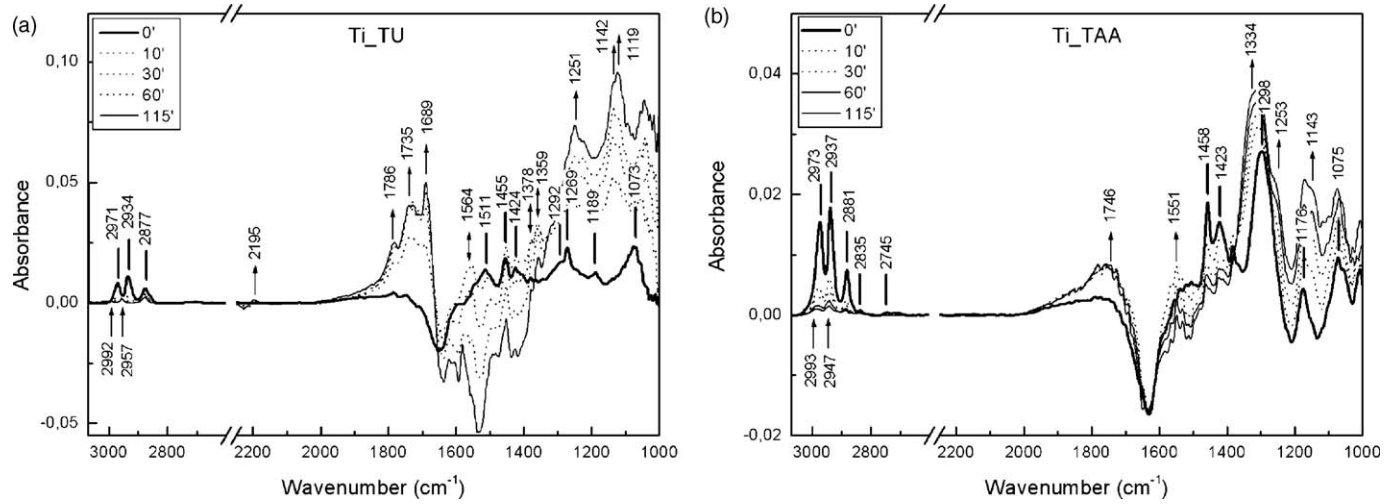

Fig. 8. DRIFT spectra of CEES in humid environment on as prepared (a) Ti_TU and (b) Ti_TAA. Spectra shown are prior to illumination and after 10, 30, 60 and 115 min of UV illumination, respectively. The arrows indicate growth or decline of absorbance vs. illumination time.

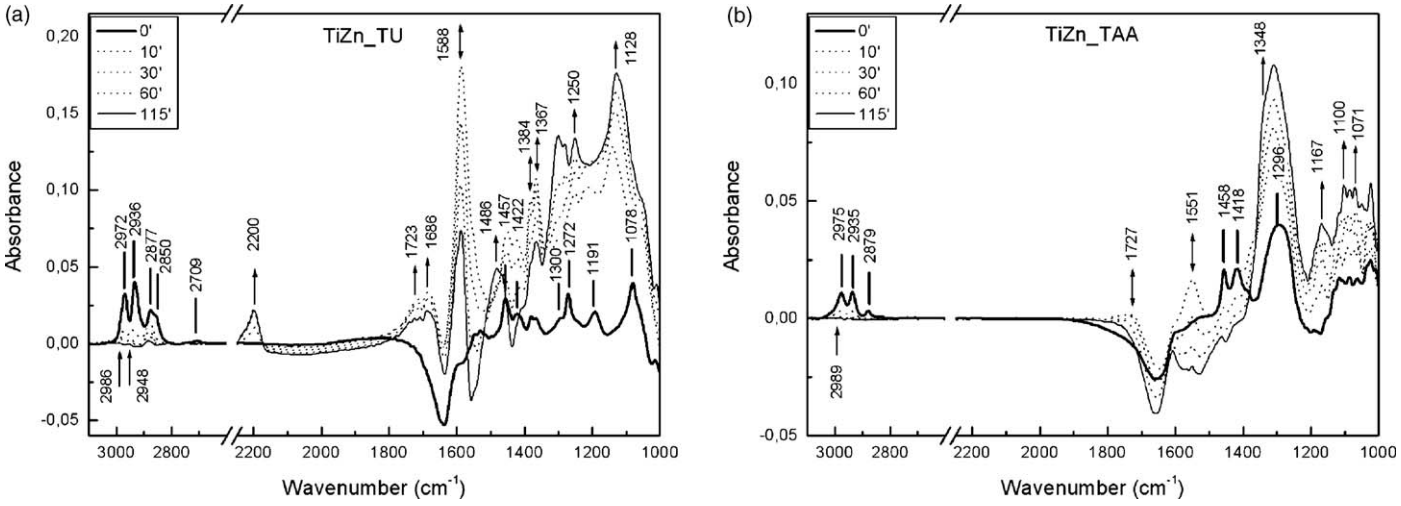

Fig. 9. DRIFT spectra of CEES in humid environment on as prepared (a) TiZn_TU and (b) TiZn_TAA. Spectra shown are prior to illumination and after 10, 30, 60 and 115 min of UV illumination, respectively. The arrows indicate growth or decline of absorbance vs. illumination time.

reason for this is due to site blocking of cation sites with water molecules that prevents formation of strongly bonded surface intermediates as evidenced by DRIFT spectra and facile reactions with hydroxyl radicals. The integral hydrocarbon absorption signal yields in general a lower reaction rate compared to the vibrational mode specific bands associated with the parent CEES molecules (Tables 2 and 3), in agreement with our previous studies [35,36]. This is particularly evident for the Zn doped samples. For example, on sample TiZn_TAA in Fig. 9 the peaks associated with the asymmetric ν(COO) mode at ca. 1550 cm^{-1} characteristic for carboxylates and bicarbonate vanishes during the measurement time, in contrast to the dry case. Looking in more detail it is seen that adsorbed CN from the photoreaction of urea residues still is present. However, this absorption band is shifted to lower wavenumbers, 2199 cm^{-1} and is much weaker compared to the dry cases (Fig. 4a) indicating a lower amount of residues present in the samples which is especially true for the pure titania sample. Since the total degradation rate as approximated by the integrated ν(C–H) band is determined by the oxidation of these intermediates [36], this implies that the total conversion rate is faster on a water covered surface (however if the water cover is too thick then the rate goes down; thus there exist an optimum water coverage. In fact, it can be shown that there exist an optimum temperature and relative humidity of the reaction gas [37]). The results presented here clearly demonstrates the difference between aqueous and gas photodegradation studies; in aqueous solutions additional reaction pathways involving reactions of H_2O with volatile sulphate species effectively contribute to the overall degradation rates. In particular, the influence of catalyst reactivity is less sensitive to pretreatment in aqueous photocatalysis studies. However, in cases where dopant atoms (here Zn) can be expected to bind strongly with residual products from synthesis, caution should also be taken in those studies.

4. Conclusions

The present study reveals that TiO_2 and Zn doped TiO_2 prepared by homogeneous hydrolysis in aqueous solution results in very different photo-reactivity depending on whether urea and thioacetamide are used as precipitating agent. In particular we have determined and identified residual synthesis products and

cleaning procedures to evaluate the intrinsic nanoparticle reactivity for the different nanoparticle systems.

We find that residues from the materials syntheses can be found in all tested samples, which are depleted in varying degree upon photoreaction, which is evident by the negative absorbance bands at 1400–1600 cm^{-1} (urea route) and 1360 cm^{-1} (thioacetamide route, or bulk S segregation from $TiOSO_4$ residues) formed during the photoreaction. Extended calcination to 24 h at 440 °C is sufficient to remove most of the urea derived surface moieties, while additional NaOH washing is necessary to remove thioacetamide residues. However, calcination leads in general to surface segregation of sulphur impurities present in the bulk which originates from the sulphate precursors ($TiOSO_4$) used in the TiO_2 particle synthesis.

It is found that the intrinsic photodegradation rates on TiO_2 particles are highest on the pure TiO_2 particles, in particular those prepared via the urea route. Zn doping results in stronger bonding of sulphur moieties and reaction intermediates on the surface and a concomitant lower photo-reactivity.

In humid environment or humidified surfaces, the effects of volatile surface residues are reduced, which is manifested in the faster kinetics of the surface species and lower concentration of surface intermediates. Similarly, the inhibiting effect of Zn bonding to surface intermediates and sulphur moieties is reduced. All samples exhibit in general improved photodegradation rates in humid environment. Our results highlight the difference between dry and solution based photocatalysis studies, and shows that both reaction pathways and rate determining steps can be very different. From an applied viewpoint our results stress and pinpoint the importance in material development of distinguishing intrinsic, material specific reactive properties from spurious effects originating from material synthesis and to device protocols that assures that appropriate reactive properties are measured.

Acknowledgements

Authors acknowledge kind financial support provided by the Academy of Sciences of the Czech Republic (Project No. AV OZ 40320502), also the Czech Science Foundation (Project No. 203/08/0335), and the Swedish Defence Materials Administration (Project No. FMV E46484).

References

[1] M.R. Hoffmann, S.T. Martin, W. Choi, D.W. Bahnemann, Chem. Rev. 95 (1995) 69.
[2] A.L. Linsebigler, G. Lu, J.T. Yates Jr., Chem. Rev. 95 (1995) 735.
[3] J. Peral, D.F. Ollis, J. Mol. Catal. A 115 (1997) 347.
[4] A. Fujishima, K. Hashimoto, T. Watanabe, TiO_2 Photocatalysis. Fundamentals and Applications, BKC, Tokyo, 1999.
[5] S. Malato, J. Blanco, A. Vidal, C. Richter, Appl. Catal. B 37 (2002) 1.
[6] O. Carp, C.L. Huisman, A. Reller, Prog. Solid State Chem. 32 (2004) 33.
[7] A.V. Vorontsov, C. Lion, E.N. Savinov, P. Smirniotis, J. Catal. 220 (2003) 414.
[8] S. Kataoka, E. Lee, M.I. Tejedor-Tejedor, M.A. Anderson, Appl. Catal. B 61 (2005) 159.
[9] D.A. Panayotov, D.K. Paul, J.T. Yates, J. Phys. Chem. B 107 (2003) 10571.
[10] D.A. Panayotov, J.T. Yates, Chem. Phys. Lett. 399 (2004) 300.
[11] K. Hashimoto, H. Irie, A. Fujishima, Jpn. J. Appl. Phys. 44 (2005) 8269.
[12] M. Matsuoka, M. Anpo, J. Photochem. Photobiol. C 3 (2003) 225.
[13] S. Bakardjieva, V. Štengl, J. Šubrt, E. Vecerníková, Solid State Sci. 7 (2005) 367.
[14] S. Bakardjieva, J. Šubrt, V. Štengl, M.J. Dianez, M. Sayagues, J. Appl. Catal. B 58 (2005) 193.
[15] V. Štengl, M. Maríková, S. Bakardjieva, J. Šubrt, F. Opluštil, M. Olšanská, J. Chem. Technol. Biotechnol. 80 (2005) 754.
[16] V. Štengl, J. Šubrt, S. Bakardjieva, A. Kalendová, P. Kalenda, Dyes Pigm. 58 (2003) 239.
[17] G. Soler-Illia, M. Jobbagy, R.J. Candal, A.E. Regazzoni, M.A. Blesa, J. Dispersion Sci. Technol. 19 (1998) 207.
[18] J. Šubrt, J. Bohácek, V. Štengl, T. Grygar, P. Bezdicka, Mater. Res. Bull. 34 (1999) 904.
[19] T. Nomura, Y. Kousaka, M. Alonso, M. Fukunaga, J. Colloid Interface Sci. 223 (2000) 179.
[20] V. Houšková, V. Štengl, S. Bakardjieva, N. Murafa, A. Kalendová, F. Opluštil, J. Phys. Chem. A 111 (2007) 4215.
[21] V. Štengl, S. Bakardjieva, N. Murafa, V. Houšková, K. Lang, Micropor. Mesopor. Mater. 110 (2–3) (2008) 370–378.
[22] V. Houšková, V. Štengl, S. Bakardjieva, N. Murafa, J. Phys. Chem. Solids 69 (7) (2008) 1623–1631.
[23] C. Martín, I. Martín, V. Rives, J. Mater. Sci. 30 (1995) 3847.
[24] C. Hägglund, B. Kasemo, L. Österlund, J. Phys. Chem. B 109 (2005) 10886.
[25] S. Brunauer, P.H. Emmett, E. Teller, J. Am. Chem. Soc. 60 (1938) 309.
[26] E.P. Barret, L.G. Joyner, P.P. Halenda, J. Am. Chem. Soc. 73 (1951) 373.
[27] O. Danek, V. Štengl, S. Bakardjieva, N. Murafa, A. Kalendová, F. Opluštil, J. Phys. Chem. Solids 68 (2007) 707.
[28] A. Kiselev, M. Andersson, A. Palmqvist, L. Österlund, J. Photochem. Photobiol. A 184 (2006) 125.
[29] A. Mattsson, M. Leideborg, K. Larsson, G. Westin, L. Österlund, J. Phys. Chem. B 110 (2006) 1210.
[30] G. Socrates, Infrared and Raman Characteristic Group Frequencies: Tables and Charts, 3rd ed., John Wiley & Sons, Chichester, 2001.
[31] P. Hauck, A. Jentys, J.A. Lercher, Appl. Catal. B 70 (2007) 91.
[32] T.L. Thompson, D.A. Panayotov, J.T. Yates, J. Phys. Chem. B 108 (2004) 16825.
[33] W.-C. Wu, L.-F. Liao, J.-S. Shiu, J.-L. Lin, Phys. Chem. Chem. Phys. 2 (2000) 4441.
[34] S.J. Teichner, M. Formenti, in: M. Schiavello (Ed.), Photoelectrochemistry, Photocatalysis, and Photoreactors, Reidel, New York, 1985, p. 457.
[35] L. Österlund, A. Mattsson, in: L. Vayssieres (Ed.), Solar Hydrogen and Nanotechnology, vol. 6340, SPIE, San Diego, 2006, p. 1.
[36] T. van der Meulen, A. Mattsson, L. Österlund, J. Catal. 251 (2007) 131.
[37] L. Österlund, patent WO 2006/126946; L. Österlund, SPIE News 10.1117/2.1200608.0328 (2006).